

## A polar low embedded in a blocking high over the Pacific Arctic

Jun Inoue,<sup>1</sup> Masatake E. Hori,<sup>1</sup> Yoshihiro Tachibana,<sup>1,2</sup> and Takashi Kikuchi<sup>1</sup>

Received 11 May 2010; revised 21 June 2010; accepted 24 June 2010; published 31 July 2010.

[1] A polar low (PL) is a short-lived phenomenon involving strong winds that occurs over polar oceans. In October 2009, the R/V *Mirai* encountered a PL with a 600-km-wide, comma-shaped cloud that developed over the Chukchi Sea. A shipboard Doppler radar and radiosondes were used to understand the fine structure of this PL. Analyses of low-level winds and the thermodynamic structure indicated that the development of the PL was decoupled from sea surface thermal forcing. The PL was likely triggered by an intrusion of a potential vorticity (PV) anomaly at the tropopause. A southerly warm advection associated with a blocking high over Alaska resulted in rapid development of the PL in front of the cold dome induced by the upper-level PV anomaly. The westerly winds after passage of the PL seemed to modify the upper-ocean structure dramatically. **Citation:** Inoue, J., M. E. Hori, Y. Tachibana, and T. Kikuchi (2010), A polar low embedded in a blocking high over the Pacific Arctic, *Geophys. Res. Lett.*, 37, L14808, doi:10.1029/2010GL043946.

### 1. Introduction

[2] Ice-free areas next to marginal ice zones are very unique places of strong temperature gradient. In such regions, the formation of small disturbances, so-called polar lows (PLs), is favored. PLs are mesoscale cyclones that develop over high-latitude oceans on horizontal scales from 200 to 1000 km. They are usually characterized by spiral- or comma-shaped clouds and strong wind speeds [Rasmussen *et al.*, 1993]. Despite much work using satellite observations, direct observation and classification of PLs has been difficult because of their temporal and spatial scales. In particular, the interaction between upper- and lower-level forcings are potentially very complex and can not easily be deduced from satellite imagery.

[3] There is a variety of mechanisms that can be important for the development and maintenance of PLs (baroclinic instability, conditional instability of the second kind (CISK) [e.g., Rasmussen, 1979], and wind-induced surface heat exchange (WISHE) [e.g., Emanuel and Rotunno, 1989]). Although there is still a debate going on over the means by which convection acts to intensify the PLs, theoretical investigations have focused on the way in which heating affects the development of them. Deveson *et al.* [2002] proposed the threefold cyclogenesis that is extension to the Petterssen and Smebye [1971] classification scheme for extratropical cyclones. Type A cyclones are characterized by low-level thermal advection with a phase locking to the

upper trough during the intensification phase. Type B cyclones are triggered by a pre-existing upper-level trough, and develop by thermal advection at a lower level. Type C cyclones heavily depend on upper-level potential vorticity (PV), with a low-level PV anomaly generated diabatically by latent heat release as a substitute for the basic state baroclinicity. Assessing the mechanisms important for PL intensification within the threefold classification, the atmospheric conditions associated with Type C candidates were found to be consistent with the characteristics of extratropical cyclones [Bracegirdle and Gray, 2008]. WISHE also seemed to dominate in a period of the intensification [Bracegirdle and Gray, 2009].

[4] From the viewpoint of air-sea interaction, the impact of PLs on the upper ocean is potentially important for heat exchange between atmosphere and ocean [Condrón *et al.*, 2008]. In addition, wind-driven Ekman transport is known to be strong in the western Beaufort and Chukchi seas [Yang, 2006]. Offshore flow in the upper layers driven by easterly winds carries heat and fresh water into the Beaufort Gyre and also leads to strong upwelling along the margins of the Chukchi and Beaufort seas. Due to the cyclonic winds of PLs, the structure of the upper ocean (temperature and salinity) could be modified by a rapid change in wind direction.

[5] PLs in the Beaufort and Chukchi seas are rare events compared to those in the North Atlantic region [Rasmussen and Turner, 2003]. However, Parker [1989] suggested that ‘Given optimum synoptic conditions during a year when ice cover is at a minimum, it should be possible for a polar low to develop over the southern Beaufort Sea.’ The recent rapid decrease in the Arctic sea-ice extent over the Pacific sector is increasing observation targets, from the sea ice itself to the changes in the ocean and atmosphere associated with changes in sea ice. Even if a ship is not an ice-breaker, it is now possible for it to reach and observe the Arctic Ocean. For example, the Japanese R/V *Mirai*, an ice-strengthened ship, has frequently entered the Arctic Ocean, particularly the ice-free region, and continues to break northernmost records (76.4°N in 2002, 76.6°N in 2004, 78.9°N in 2008, and 79.0°N in 2009). In October 2009, we encountered a PL over the Chukchi Sea during an Arctic Ocean cruise of the R/V *Mirai*. Using the shipboard radiosonde and radar systems along with oceanographic instruments, we studied the fine structure of the PL, its development mechanism, and its impact on the upper ocean.

### 2. Observations by the R/V *Mirai*

[6] An Arctic cruise was conducted by the R/V *Mirai* over the Chukchi and Beaufort seas from 7 September to 15 October 2009 ([http://www.godac.jamstec.go.jp/cruisedata/mirai/e/MR09-03\\_leg2.html](http://www.godac.jamstec.go.jp/cruisedata/mirai/e/MR09-03_leg2.html)). During the cruise, an intensive meteorological observation period was set up from 7 to

<sup>1</sup>Research Institute for Global Change, Japan Agency for Marine-Earth Science and Technology, Yokosuka, Japan.

<sup>2</sup>Climate and Ecosystem Dynamics Division, Mie University, Tsu, Japan.

10 October over the Chukchi Sea where the sea surface temperature (SST) gradient along 72.5°N line was large (e.g., 1 K per 10 km). In this period, 3-hourly GPS radiosonde observations (Vaisala RS92-SGPD) were performed at 0.5° latitude and 2° longitude intervals along the ship tracks in the 71.5–73.5°N, 162–168°W region. In this study, we mainly analyzed the data from 162°W section.

[7] Shipboard C-band Doppler radar observation (RC-52B, Mitsubishi Electric Co. Ltd., Japan) was simultaneously performed. During the observation, a volume scan consisting of 21 plan position indicators (PPI) was made every 10 minutes (detection range: 160 km). Meanwhile, a surveillance PPI scan at an elevation angle of 0.5 was performed every 30 minutes (detection range: 300 km). The velocity-azimuth display (VAD) method [e.g., *Browning and Wexler*, 1968] was used to estimate horizontal wind fields from the Doppler velocity. The correlation between the radiosonde and VAD winds (1800 UTC on 9 October, 0000 UTC and 0300 UTC 10 October) exceeded 0.90 below 4 km, suggesting that the VAD winds at 10-minute temporal resolution are highly valuable for investigations of cloudy boundary layers.

[8] To study the synoptic situation, Advanced Very High-Resolution Radiometer (AVHRR) satellite images were used in this study. Expendable conductivity-temperature-depth (XCTD) sensors and processing equipment (Tsurumi-Seiki Co., Ltd., Yokohama, Japan) and shipboard CTD sensors were used to measure temperature and conductivity (and hence salinity) from the sea surface to the bottom at the same locations as the radiosonde stations. Ancillary datasets included shipboard meteorological surface observations and Japanese reanalysis data from the Japan Meteorological Agency (JMA Climate Data Assimilation System: JCDAS) [*Onogi et al.*, 2007].

### 3. Polar Low Over the Chukchi Sea

[9] Figure 1 shows the temporal evolution of the PL in four selected satellite images overlaying the closest radar reflectivity. The comma-shaped cloud started to develop around 2000 UTC 9 October (Figure 1b) near Point Barrow, Alaska, accompanying outer cloud bands which appeared in advance (Figure 1a). The PL developed very quickly in a few hours (Figure 1c) and reached a matured stage with northward movement toward the marginal ice zone (Figure 1d). On the basis of the brightness temperature (less than  $-40^{\circ}\text{C}$ ), it was obvious that the comma-shaped cloud developed at the upper troposphere.

[10] Time-height cross sections of the VAD horizontal winds just above the radar are shown in Figure 2. The system can be divided into two periods. The first period, from 1400 to 2000 UTC 9 October, during which the ship was positioned under the outer cloud bands of the PL, was characterized by moderate southeasterly winds above 2 km. This system moved northward with  $10.4\text{ m s}^{-1}$ . The latter period, from 2000 UTC 9 October to 0300 UTC 10 October, under the central region of the PL, was characterized by the opposite zonal wind direction after the passage of the center on 0100 UTC 10 October. This system moved  $16.2\text{ m s}^{-1}$ , which was consistent with an upper meridional wind component (i.e., the steering level is above 2.5 km (Figure 2c)).

[11] One interesting aspect of the development was the decoupling between the lower and upper layers. For example,

the zonal wind component indicated easterlies greater than  $10\text{ m s}^{-1}$  below the 0.5-km level, while the meridional wind component below 2 km was not modified after passage of the PL. Although the ship crossed the SST front on 1930 UTC (Figure 2d), the lower boundary layer was not modified.

[12] Comparing the profiles of air temperature and humidity obtained by the radiosondes (Figures 3a–3c), the lower structures were the same on the outside (Figures 1a and 1b) and inside (Figure 1c and 1d) of the PL. In other words, stable temperature profiles and strong humidity inversion occurred up to the 2-km level. This feature arose from the persistent strong east-southeasterly winds that originated from the sea ice area (i.e., cold and dry advection below the 2-km level). Due to the strong vertical wind shear under the condition of small air-sea temperature differences, the turbulent kinetic energy (TKE) structure of the lower layer was maintained by strong shear production (i.e., a shear-driven mechanism) [e.g., *Inoue et al.*, 2005]. Above the layer, a relatively large mixing ratio amount (over  $4\text{ g kg}^{-1}$ ) was observed, suggesting warm advection there. However, the temperature profiles outside and inside the PL in the upper troposphere were significantly different. In the outer band, the height of the tropopause was 11 km, while inside the PL the tropopause height dropped to 7.5 km. In addition, the air temperature (Figure 3a) decreased by 5 K in the middle troposphere (e.g., the 5-km level) and 10 K in the upper troposphere (the 7-km level), implying a response to advection of the positive upper-level potential vorticity (UPV) anomaly [*Hoskins et al.*, 1985].

[13] Figure 3d shows the time-height cross section of potential temperature and zonal winds obtained by 3-hourly intensive radiosonde observations during the passage of the PL. At the matured stage of the PL (i.e., around 0300 UTC 10 October, when the sea level pressure dropped to 1012.5 hPa), the upper troposphere was covered with a cold dome (see, e.g., 312 K contour in Figure 3d). Considering that the PL was moving northward and had a cyclonic wind field around a cold dome, this situation seems to be the case of an UPV intrusion. The induced upward motion in advance of the approaching UPV was very likely to generate precipitating clouds.

[14] In our case, the SST gradient over the Chukchi Sea (Figure 3e) might have been very favorable for baroclinic development (a Type A cyclone). However, the surface air temperature seemed not to be affected by the UPV, but modified by the SST (Figure 3e), because of the relatively cold advection from the ice-covered area. This suggested that the effect of the UPV intrusion was limited to the region above 2 km. In other words, the high static stability in the lower layer below 2 km (Figures 3a and 3b) prevented communication between the UPV and low-level features forced by strong SST gradients near the ice edge.

[15] Figure 1e shows the height and air temperature fields at 500 hPa and PV fields larger than 2 PVU at the  $\theta_{310\text{K}}$  level based on the JCDAS reanalysis data. The PL formation was located in front of the higher PV anomaly area (PV > 2 PVU) with a cold core ( $-24^{\circ}\text{C}$ ) over the Chukchi Sea. There was a strong southerly warm advection over Alaska associated with a blocking high, suggesting the generation of convective clouds (i.e., the outer bands of the PL) associated with instability created by a layer of warm advection below the mid-tropospheric cold core. A consequent lower-level PV

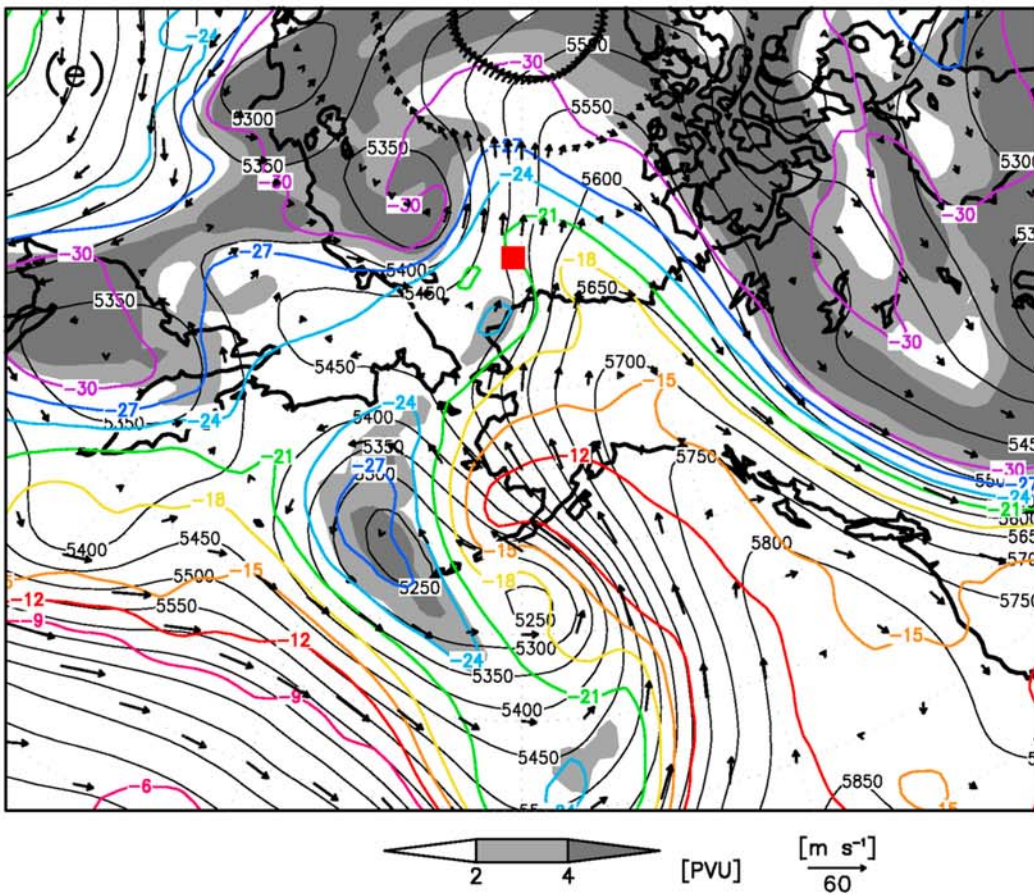
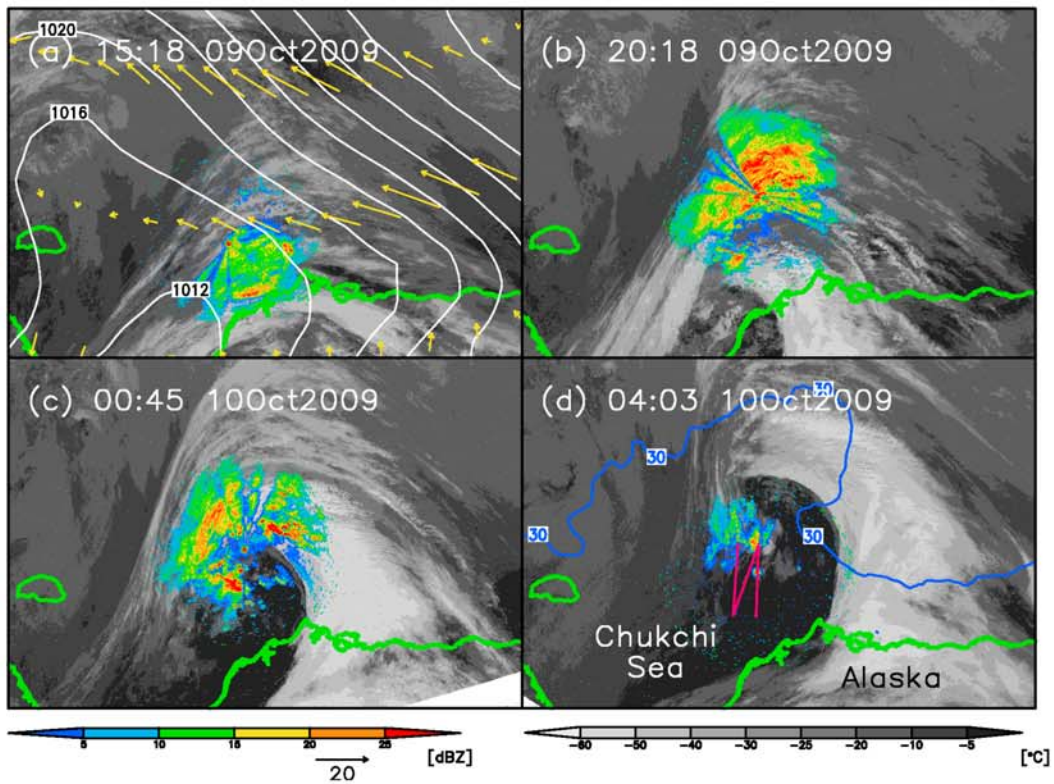
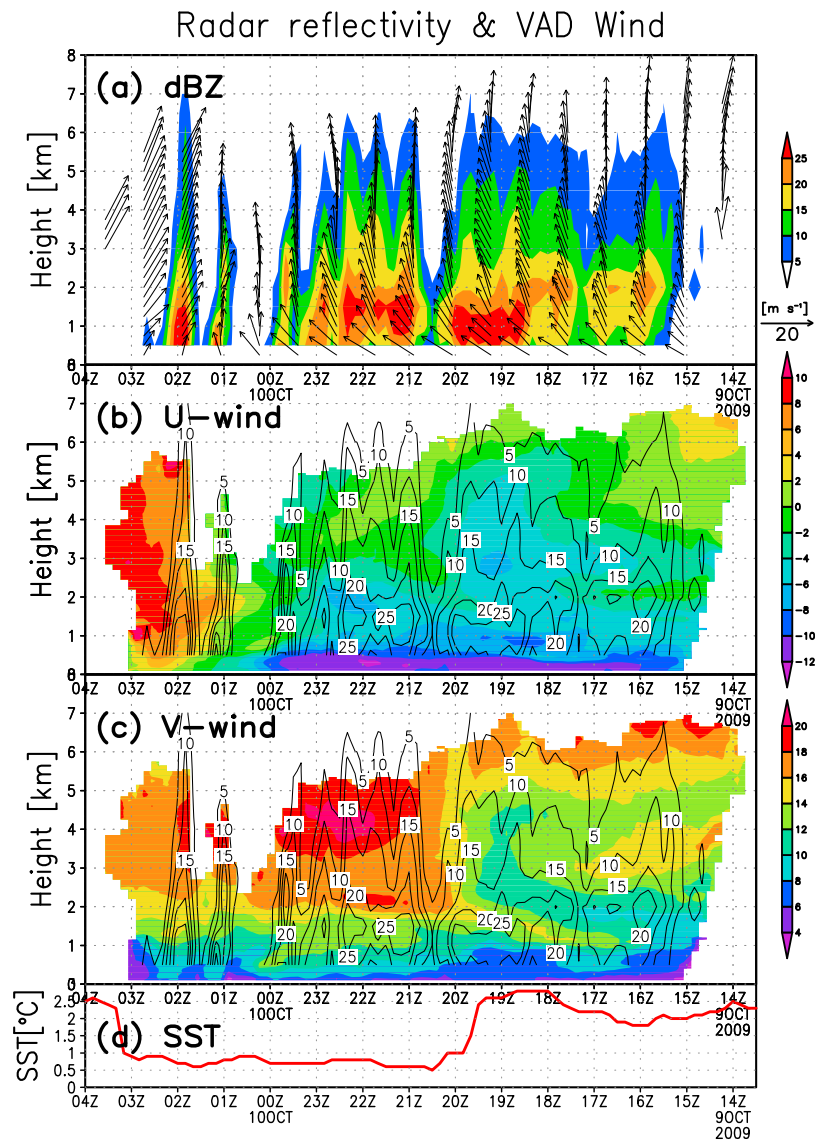


Figure 1



**Figure 2.** Time-height cross sections of (a) radar reflectivity (dBZ: shade) and VAD horizontal wind ( $\text{m s}^{-1}$ : vector), (b) zonal, and (c) meridional wind components (shade), and radar reflectivity (contour). (d) Time series of sea surface temperature ( $^{\circ}\text{C}$ ). The northern side of the PL is the right-hand side.

anomaly presumably resulted from latent heat release (i.e., Type C mechanism). It is consistent that this type of cyclone consisted of a comma-shaped cloud in its developing stage, as Deveson *et al.* [2002] described. Although some PLs are related to a strong blocking situation in the Nordic seas (anomalously high pressure over Iceland and a synoptic-scale low-pressure anomaly over the Barents Sea), the centers of PLs are usually located on the low pressure side (e.g., a composite analysis by Blechschmidt *et al.* [2009],

and a case study by Brümmer *et al.* [2009]). Therefore, our case, a PL embedded in a blocking high, is unique.

#### 4. Summary and Discussion

[16] Our Doppler radar and radiosonde observations showed rapid PL development on 9–10 October 2009 over the Chukchi Sea. The UPV likely works as a trigger for PL formation. Our findings provide direct evidence that a PL

**Figure 1.** Brightness temperature ( $^{\circ}\text{C}$ ) of AVHRR images and radar reflectivities (dBZ) at (a) 1518 UTC and (b) 2018 UTC 9 October, and (c) 0045 UTC and (d) 0403 UTC 10 October 2009. Sea level pressure (hPa: contour) and 10-m wind (vectors) fields on 1800 UTC 9 October were shown in Figure 1a. The ship track from 0000 UTC 9 October ( $73.5^{\circ}\text{N}$ ,  $164^{\circ}\text{W}$ ) to 1200 UTC 10 October ( $71.5^{\circ}\text{N}$ ,  $162^{\circ}\text{W}$ ) is shown by a thin pink line in Figure 1d. The ice concentration (30%) derived from Advanced Microwave Scanning Radiometer - Earth Observing System (AMSR-E) data is also depicted by the blue contour. (e) Isentropic distributions of potential vorticity at the 310-K level (shading), air temperature ( $^{\circ}\text{C}$ : color contour), geopotential height (m: black contour), and wind fields (vector) at the 500-hPa level on 0000 UTC 10 October 2009. The red square denotes the position of the R/V *Mirai*.

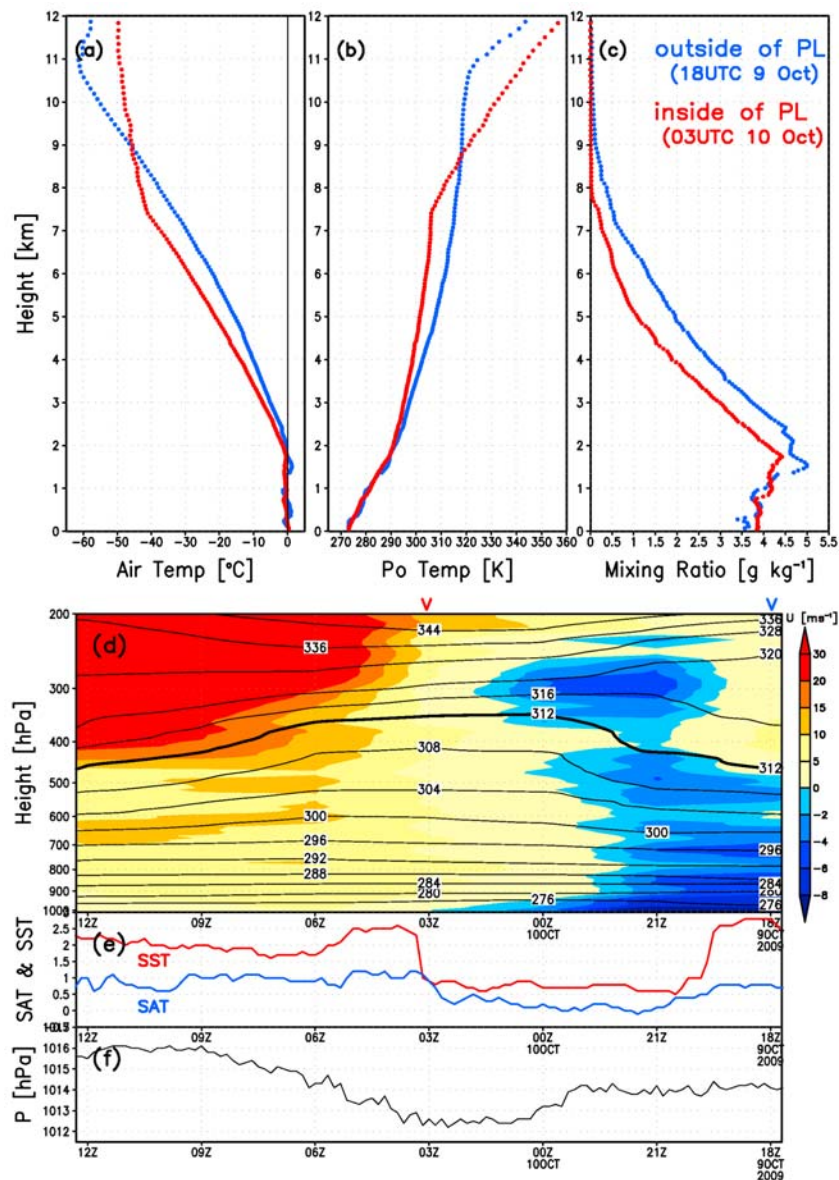


**Figure 3.** Vertical profiles of (a) air temperature ( $^{\circ}\text{C}$ ), (b) potential temperature (K), and (c) vapor mixing ratio ( $\text{g kg}^{-1}$ ). Red and blue lines denote the profiles for the outside (1800 UTC 9 October) and inside (0300 UTC 10 October) of the PL, respectively. Time–height cross section of Figure 3d potential temperature (contour) and zonal wind (shading) observed by radiosondes. The timing of soundings in Figures 3a–3c are indicated by ‘v’. Time series of (e) temperatures of the sea surface (red) and air (blue), and (f) sea level pressure observed by the R/V *Mirai*. The ship’s speed was almost constant ( $18.5 \text{ km h}^{-1}$ ). The northern side of the PL is the right-hand side.

can be formed without thermal forcing near the sea surface (i.e., a Type C cyclone).

[17] However, another type of PLs were detected by satellite images on 7 September, and 2 and 17 October (figure not shown). The strong SST gradient over the Chukchi Sea corresponding to the sea-ice retreat during late summer is presumably favorable for generation of Type A cyclones by baroclinic dynamics. Recent easterly wind anomalies along the Beaufort High during late summer associated with the Arctic Dipole [e.g., Overland and Wang, 2010] might have strengthened the SST front over the Chukchi Sea due to Ekman transport, increasing the generation of PLs.

[18] Yang [2006] demonstrated that offshore flow induced by easterly winds during fall and winter carries heat and fresh water into the Beaufort Gyre and leads to strong upwelling along the margins of the Chukchi and Beaufort seas. In addition, the strong easterly winds over the southern Beaufort Sea resulting from synoptic storms likely drive individual upwelling events. This can be seen from mooring records from the Beaufort slope [e.g., Aagaard *et al.*, 1981]. Rapid changes in wind direction associated with the passage of PLs are also a suitable way to investigate the response of the upper ocean. Figure 4 shows latitude–height cross sections of the atmosphere (potential temperature and zonal wind) and ocean (water temperature and salinity) before

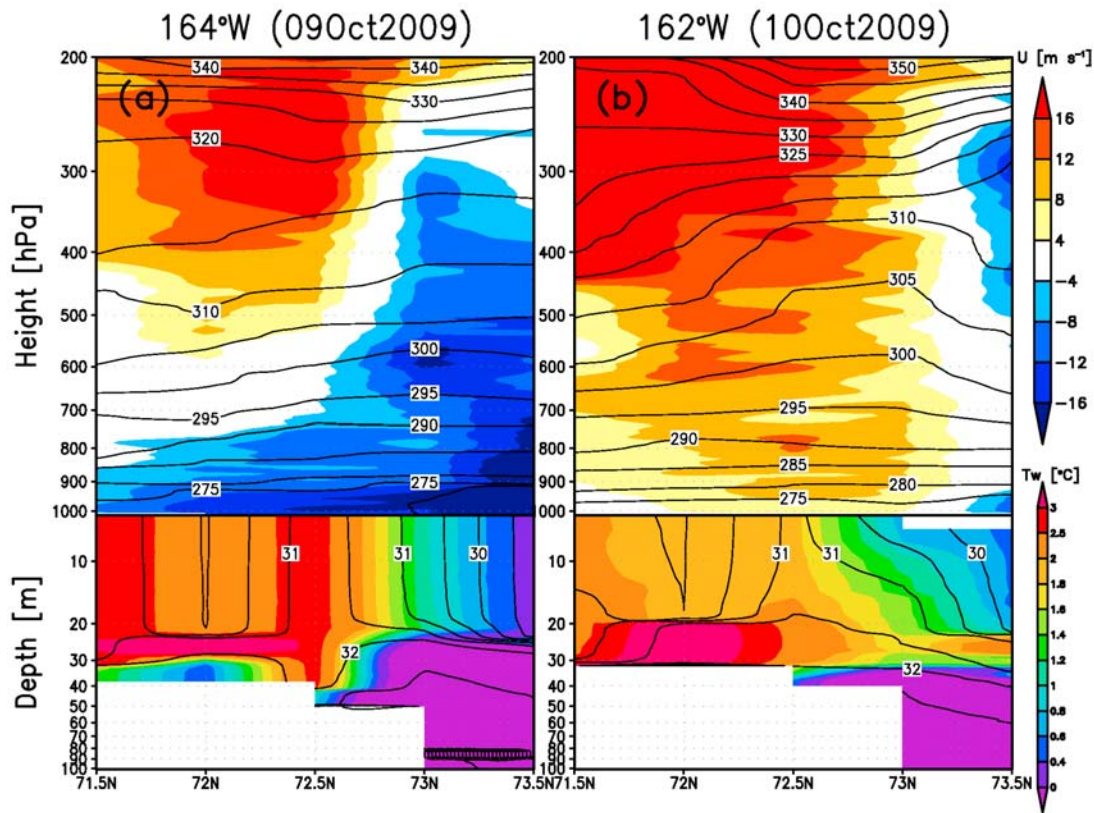


**Figure 4.** Latitude-height cross sections of (top) zonal wind ( $\text{m s}^{-1}$ : shade) and potential temperature (K: contour) and (bottom) water temperature ( $^{\circ}\text{C}$ : shade) and salinity (psu: contour) (a) along  $164^{\circ}\text{W}$  on 9 October and (b) along  $162^{\circ}\text{W}$  on 10 October 2009.

( $164^{\circ}\text{W}$  line) and after ( $162^{\circ}\text{W}$  line) the PL passage. From a two-dimensional perspective, the persistent easterly wind from the sea-ice area associated with the low-level high pressure system over the Beaufort Sea (Figure 1a) is favorable for upwelling. This presumably results in formation of the ocean mixed layer by wind-driven Ekman transport, and raises the Arctic halocline over the slope at depth about 25 m (Figure 4a). After passage of the PL, however, westerly (i.e., downwelling-favorable) wind transports the cold and fresh water from the northern region, perhaps resulting in the southward tilting of the isotherms (Figure 4b).

[19] Strong, rapidly changing winds from easterlies to westerlies probably disturb the surface stratification, preventing the upper layer from freezing during early winter. To understand the causal relationship between the development of PLs and the responses of the ocean surface and sea-ice formation, frequent *in situ* observations of PLs over the SST front as well as three-dimensional numerical experiments would be desirable in the near future.

[20] **Acknowledgments.** We are greatly indebted to S. Sueyoshi, S. Okumura, N. Nagahama, R. Kimura, and M. Ito for conducting radiosonde and radar observations. The authors would like to thank officers and crews of the R/V *Mirai*. Radar analysis was done by using the Draft tool developed by JMA/MRI. Comments from anonymous reviewers were very helpful.

## References

Aggaard, K., L. K. Coachman, and E. C. Carmack (1981), On the halocline of the Arctic Ocean, *Deep Sea Res.*, **28**, 529–545.

- Blechschmidt, A.-M., S. Bakan, and H. Grafl (2009), Large-scale atmospheric circulation patterns during polar low events over the Nordic seas, *J. Geophys. Res.*, **114**, D06115, doi:10.1029/2008JD010865.
- Bracegirdle, T. J., and S. L. Gray (2008), An objective climatology of the dynamical forcing of polar lows in the Nordic seas, *Int. J. Climatol.*, **28**, 1903–1919.
- Bracegirdle, T. J., and S. L. Gray (2009), The dynamics of a polar low assessed using potential vorticity inversion, *Q. J. R. Meteorol. Soc.*, **135**, 880–893.
- Browning, K. A., and R. Wexler (1968), The determination of kinematic properties of a wind field using Doppler radar, *J. Appl. Meteorol.*, **7**, 105–113.
- Brümmer, B., G. Müller, and G. Noer (2009), A polar low pair over the Norwegian Sea, *Mon. Weather Rev.*, **137**, 2559–2575.
- Condron, A., G. R. Bigg, and I. A. Renfrew (2008), Modeling the impact of polar mesocyclones on ocean circulation, *J. Geophys. Res.*, **113**, C10005, doi:10.1029/2007JC004599.
- Deveson, A. C. L., K. A. Browning, and T. D. Hewson (2002), A classification of FASTEX cyclones using a height-attributable quasi-geostrophic vertical-motion diagnostic, *Q. J. R. Meteorol. Soc.*, **128**, 93–118.
- Emanuel, K. A., and R. Rotunno (1989), Polar lows as Arctic hurricanes, *Tellus, Ser. A*, **41**, 1–17.
- Hoskins, G. J., M. E. McIntyre, and A. W. Robertson (1985), On the use and significance of isentropic potential vorticity maps, *Q. J. R. Meteorol. Soc.*, **111**, 877–946.
- Inoue, J., B. Kosović, and J. A. Curry (2005), Evolution of a storm-driven cloudy boundary layer in the Arctic, *Boundary Layer Meteorol.*, **117**, 213–230.
- Onogi, K., et al. (2007), The JRA-25 reanalysis, *J. Meteorol. Soc. Jpn.*, **85**, 369–432.
- Overland, J. E., and M. Wang (2010), Large-scale atmospheric circulation changes are associated with the recent loss of Arctic sea ice, *Tellus, Ser. A*, **62**, 1–9.
- Parker, M. N. (1989), Polar lows in the Beaufort Sea, in *Polar and Arctic Lows*, edited by P. F. Twitchell, E. A. Rasmussen, and K. L. Davidson, pp. 323–330, A. Deepak, Hampton, Va.
- Petterssen, S., and S. J. Smebye (1971), On the development of extratropical cyclones, *Q. J. R. Meteorol. Soc.*, **97**, 457–482.
- Rasmussen, E. (1979), The polar low as an extratropical CISK disturbance, *Q. J. R. Meteorol. Soc.*, **105**, 531–549.

Rasmussen, E. A., and J. Turner (Eds.) (2003), *Polar Lows: Mesoscale Weather Systems in the Polar Regions*, 612 pp., Cambridge Univ. Press, Cambridge, U. K.

Rasmussen, E. A., J. Turner, and P. F. Twitchell (1993), Report of a workshop on applications of new forms of satellite data in polar low research, *Bull. Am. Meteorol. Soc.*, 74, 1057–1073.

Yang, J. (2006), The seasonal variability of the Arctic Ocean Ekman transport and its role in the mixed layer heat and salt fluxes, *J. Clim.*, 19, 5366–5387.

---

M. E. Hori, J. Inoue, T. Kikuchi, and Y. Tachibana, Research Institute for Global Change, Japan Agency for Marine–Earth Science and Technology, 2–15 Natsushima-cho, Yokosuka 237-0061, Japan. (jun.inoue@jamstec.go.jp)